ChemComm

Accepted Manuscript

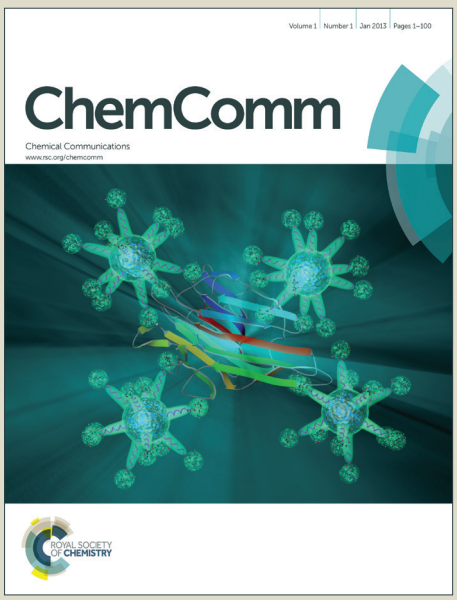

ROYAL SOCIETY OF CHEMISTRY

www.rsc.org/chemcomm

ChemComm

RSCPublishing

COMMUNICATION

In situ Raman Spectroscopic Measurement of Near-Surface Proton Concentration Changes during Electrochemical Reactions

Cite this: DOI: 10.1039/x0xx00000x

Received 00th January 2012,
Accepted 00th January 2012

DOI: 10.1039/x0xx00000x

www.rsc.org/

D.-J. Chen and Y. Y. J. Tong*

We report a simple *in situ* Raman spectroscopic measurement of near-surface proton concentration changes at commercial Pt black nanoparticle surfaces using the well-known methanol oxidation, oxygen reduction, Pt oxidation and reduction reactions as the representative illustrating examples.

Proton concentration (acidity), or pH values in general, is one of the key parameters that govern the reaction kinetics, mechanisms and rates for electrochemical (EC) reactions such as corrosion or anodic oxidation or cathodic reduction in fuel cells that take place at an electrode/electrolyte interface.[1-6] As the local near-surface proton concentration is expected to be different from that of bulk electrolyte during reactions of which the reaction rate is faster than the proton diffusion rate[1, 2, 7] and most if not all reactions in fuel cell[8-10] involve both proton transfer and electron transfer ($R \rightarrow O + H^+ + e^-$), measuring the near-surface proton concentration changes during the EC reactions is clearly of fundamental importance in unraveling the associated reaction mechanism(s). While electron transfer can be measured directly by the EC currents as the reactions take place, measuring the associated near-surface proton concentration (pH) changes is still far from straightforward. Scanning EC microscope (SECM) based pH microprobe was previously used potentiometrically[11] or voltammetrically[12] to measure changes in near-surface pH value, so were the rotating ring disk electrodes (RRDE).[13, 14] However, each of these methods has its own limitations: either pH sensitive membrane tip[11] or special proton sensing material[13, 14] is needed, or proton is required to be either the reactant or product of the tip-probing reaction.[12] These special requirements limit the scope of their applications. Moreover, the SECM and RRDE methods measure the H^+ flux in the solution rather than the near-surface proton concentration changes.

In this Communication, we report a simple Raman spectroscopy based *in situ* method (see Electronic Supporting Information–ESI for experimental details), as illustrated schematically in Figure 1. The method can measure the near-surface proton concentration changes during methanol (MeOH) oxidation or oxygen reduction reaction (MOR or ORR) or Pt surface oxidation and its subsequent reduction in normal acidic condition (0.02 ~ 0.5 M $HClO_4$) on commercial (Johnson-Matthey) Pt black nanoparticles (NPs) without introducing a third-party pH-probing species as done previously.[15-18] More specifically, we discovered that the anion ClO_4^- of the supporting electrolyte, which has an easily observable vibrational band at ~ 930 cm^{-1}, can be used as an *in situ* molecular reporter of the near-surface pH value, i.e., the proton concentration, changes as the stringent requirement of local (~3 nm) electroneutrality in the electrolyte[19] ensures that any changes in near-surface proton concentration [H^+] in a volume probed by the Raman laser will be balanced immediately by its counter-ion ClO_4^-. As aqueous solution of $HClO_4$ is a widely used supporting electrolyte, we expect that the *in situ* method reported here will find broader applications than previously reported methods can offer.

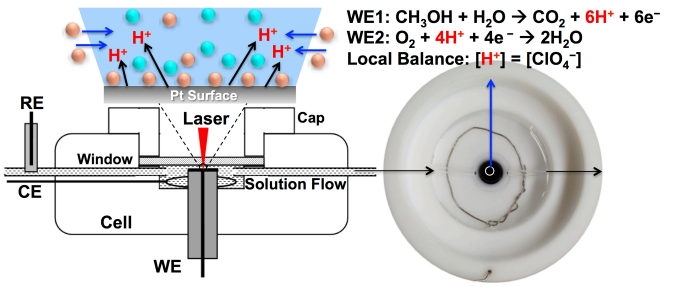

Fig. 1. Schematic Illustration of the *in situ* electrochemical Raman flow cell and charge balance during reactions on Pt surface (left). The H^+ and ClO_4^- ions are represented by cyan and orange balls respectively. The photographic top view of the real cell is shown on the right, with the center as the working electrode for MOR or ORR and the concentric Pt wire loop as the counter electrode.

As shown schematically in the left of Figure 1, the Raman laser was focused onto the Pt NPs supported on a polished glassy carbon (GC) electrode through a transparent quartz window. The actual home-made three-electrode *in situ* EC Raman follow cell is shown in the right of Figure 1. The distance of ~2 mm between the Raman window and electrode surface ensures free diffusion of H^+ and ClO_4^- in the cell. The local information was probed by a ~3 μm laser spot whose

dimension is much larger than the Debye-Hückel length of the electrolyte (<~3 nm)[19] and under which the reactions took place to produce or consume protons, such as MOR (WE1) for the former or ORR (WE2) for the latter. Although proton does not have Raman bands, its counter-ion, ClO_4^-, in $HClO_4$ supporting electrolyte does exhibit an easily observable Raman vibrational band at ~930 cm^{-1} for ν(Cl=O) stretching (Figure S1a in the ESI). As the dimension of the probing laser spot is ~1000 time larger than the Debye-Hückel length of the electrolyte (*vide supra*), we expect that the electroneutrality will be achieved and maintained over the time of a given *in situ* Raman spectral scan (180 s) at a given electrode potential so that $[H^+] = [ClO_4^-]$. That is, by measuring changes in $[ClO_4^-]$, we can infer quantitatively changes in $[H^+]$. Indeed, the feasibility of this approach is demonstrated by the control and calibration experiments as shown in Figure S1 and Table S1 in which the Raman spectra of ClO_4^- were measured at 0 V (vs. Ag/AgCl 1M, Bioanalytical) as a function of the bulk concentration of pristine $HClO_4$ electrolytes (see Figure S2 for the cyclic voltammograms (CVs) of the Pt black NPs recorded in these electrolytes). As can be seen, a Beer's Law-like linear relationship (R^2=0.9996, see the inset in Figure S1) between the $[H^+]$ of the bulk electrolyte and the $[ClO_4^-]$ as measured by the normalized Raman spectra (Figure S1b) from 0.01 M to 0.5 M. To substantiate the practical viability of the proposed method, we discuss below three representative cases.

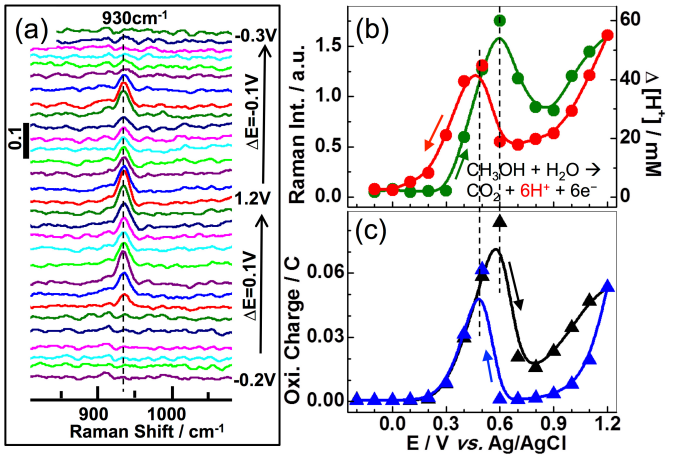

Fig. 2. (a) Potential-dependent normalized Raman spectra of MOR in 0.1 M $HClO_4$ + 0.5 M CH_3OH. (b) Potential-dependent integrated Raman band intensities (left axis) and the corresponding $\Delta[H^+]$ (right axis) during the MOR. (c) Oxidation charges for each applied potential step.

The first case is the MOR on the Pt black NPs surface in 0.1 M $HClO_4$ + 0.5 M MeOH that produces protons via reaction:

$$CH_3OH + H_2O \rightarrow CO_2 + 6H^+ + 6e^- \quad (1)$$

Per eq. (1), an increase or a decrease in MOR will cause an increase or a decrease in the near-surface $[H^+]$. Such variation is indeed observed in Figure 2a where the normalized (vs. the spectrum recorded at the initial -0.3 V) *in situ* Raman spectra of the ClO_4^- are plotted as a function of the stair-step electrode potential as the latter increased from -0.3 V to 1.2 V (positive potential scan–PPS) then returned to -0.3 V (negative potential scan–NPS) with an incremental potential step = 0.1 V. During this potential excursion, the integrated Raman band intensity of the ClO_4^- at ~930 cm^{-1} (Figure 2b) varied in almost the same pattern as the integrated charge of the MOR over the length (180 s) of each stair-step potential (Figure 2c, see Figure S3 for the charge integration), demonstrating the quantitative nature of the measurements. The corresponding changes in $[H^+]$, as calculated by the linear relationship established in the inset of Figure S1, is shown against the right axis in Figure 2b. The maximum increases in near-surface $[H^+]$ for PPS at 0.6 V and NPS at 0.5 V are 60 mM and 45 mM, respectively, during the MOR. Compared to the initial (bulk) $[H^+]$ of 100 mM (Table S1), they represent the MOR-induced near-surface $[H^+]$ increases of 60% and 45%, respectively, which are significant changes in the near-surface $[H^+]$. After the potential excursion returned to the initial value of -0.3 V, the near-surface $[H^+]$ also returned back to the initial base point as the MOR was shut down there and no protons were produced anymore (Figure 2b and 2c).

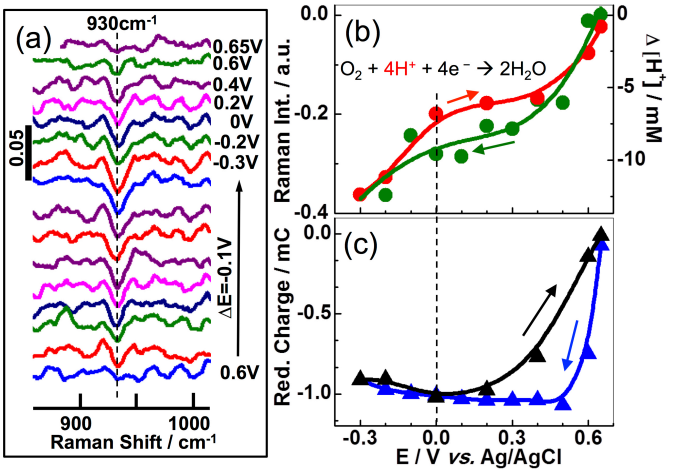

Fig. 3. (a) Potential-dependent normalized Raman spectra of ORR in O_2-saturated 0.1 M $HClO_4$. The flowing rate was 4ml/min. (b) Potential-dependent integrated Raman band intensities (left axis) and corresponding $\Delta[H^+]$ (right axis) during the ORR. (c) Reduction charges for each applied potential step.

The second case is the ORR on the Pt black NPs surface in an O_2-saturated 0.1 M $HClO_4$ electrolyte that consumes protons via reaction:

$$O_2 + 4H^+ + 4e^- \rightarrow 2H_2O \quad (2)$$

The consumption of protons in eq. (2) will lead to a decrease in near-surface $[H^+]$. Figure 3a presents the *in situ* normalized Raman spectra (vs. the one taken at the initial 0.65 V) acquired during the NPS (0.65 V to -0.3 V) and PPS (-0.3 V to 0.65 V) in the O_2-saturated 0.1 M $HClO_4$ electrolyte. The negative amplitude of the Raman band of ClO_4^- at 930 cm^{-1} in Figure 3a signifies the consumption of protons, in agreement with eq. (2). The integrated Raman band intensity of ClO_4^- (left axis) and the corresponding changes in $[H^+]$ (right axis) as a function of the stair-step electrode potential are shown in Figure 3b, and in Figure 3c are the integrated charges of ORR over the length (180 s) of each stair-step potential (see Figure S4). Overall, the signal-to-noise ratio in Figure 3a is worse than that in Figure 2a as the saturated O_2 concentration (~0.25 mM) is 80 times smaller than that of MeOH. Still, the consumption of protons for both the NPS (green) and PPS (red) is reflected in the decrease in near-surface $[H^+]$ (Figure 3b) that mimicked (although not identical) the variations in the reduction of charges except for the potential region below 0.0 V (Figure 3c). The latter deviation could be rationalized by the additional hydrogen adsorption or desorption on the Pt surface that took place in that potential region (Figure S2).[1, 7]: the adsorption consumed more protons at the surface leading to the observed further decrease and the desorption led to a faster increase in

near-surface [H^+]. However, the charges consumed in this adsorption/desorption, 0.14 mC, is smaller than the detection limit as indicated by the oxidation of a monolayer of adsorbed CO (*vide infra*), which implies a still unknown process that was involved. Notice that the change in the near-surface [H^+] during the potential excursion of the ORR was ~ 10 mM, which is much smaller than that during the MOR (~60 mM).

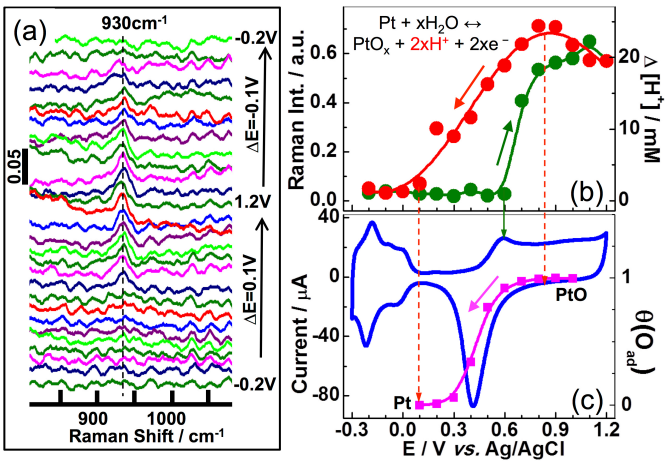

Fig. 4. (a) Potential-dependent normalized Raman spectra in pristine Ar-saturated 0.1 M $HClO_4$ electrolyte. (b) Potential-dependent integrated Raman band intensities (left axis) and the corresponding $\Delta[H^+]$ (right axis) for the Pt surface oxidation (green) an reduction (red). (c) Normal CV (blue) of the Pt NPs 0.1 M $HClO_4$ (left axis) and the corresponding reduction in the oxygen coverage during the negative potential scanning (magenta circles, right axis). The oxygen coverage was calculated by the reduction charges assuming PtO is the oxide form.

The last case is the EC oxidation of the Pt NPs surface and its subsequent oxidation during the normal CV in pristine 0.1 M $HClO_4$ electrolyte dictated by reactions

$$Pt + xH_2O \rightarrow PtO_x + 2xH^+ + 2xe^- \quad (3)$$

$$PtO_x + 2xH^+ + 2xe^- \rightarrow Pt + xH_2O \quad (4)$$

where x indicates the uncertainty about the exact oxidation state of Pt during the Raman measurements as a given potential was held for 180s for recording the Raman spectrum. It is also highly likely that the Pt oxidation went deeper than the surface during the Raman measurements. Figure 4a shows the normalized (vs. the Raman spectrum recorded at the initial -0.3 V) *in situ* Raman spectra of ClO_4^- for the oxidation (PPS) of the Pt black NPs surface and reduction (NPS). The integrated Raman band intensity (left axis) and the corresponding change in near-surface [H^+] (right axis) as a function of stair-step potential are presented in Figure 4b. The onset of the increase in near-surface [H^+] during the PPS (green circles) overlaps with the initiation of surface oxidation, eq. (3), as shown by the blue CV in Figure 4c and indicated by the vertical green arrow. For the NPS (red circles), that the $\Delta[H^+]$ continued to increase initially indicates the continuous surface oxidation. The maximum in $\Delta[H^+]$ coincided with the onset of the reduction of the PtO_x as indicated by the right red vertical arrow. Beyond that point further negatively the $\Delta[H^+]$ decreased as the PtO_x was being reduced, eq. (4), and eventually became zero when the PtO_x was fully reduced (the magenta circles in Figure 4c) as indicated by the left red vertical arrow.

However, the method failed to detect the changes in near-surface [H^+] produced by the oxidation of a monolayer of pre-adsorbed gaseous CO on the Pt black NPs surface, $CO + H_2O \rightarrow CO_2 + 2H^+ + 2e^-$, which consumed 0.26 mC of charges. The latter sets a detection limit of the method and also explains why $\Delta[H^+]$ was not detected for the hydrogen adsorption/desorption process. As to the Pt oxidation/reduction, it is not a monolayer process. That is, the Pt oxidation can continue into the bulk and generate more protons.

Conclusions

In summary, we have discovered that the ClO_4^- in $HClO_4$-based electrolytes can be used as a simple and effective *in situ* molecular Raman reporter that can probe rather *faithfully* the changes in near-surface [H^+] during EC reactions. This is enabled by that (1) the ClO_4^- has an easily observable Raman band at 930 cm^{-1} and (2) the stringent electroneutrality requirement in solution electrolytes[19] ensuring [ClO_4^-] = [H^+]. Its investigative power and technical robustness have been tested and demonstrated by the three discussed representative cases: MOR for proton generation, ORR for proton consumption, and Pt surface oxidation and its subsequent reduction for both proton generation and consumption. Although the measured proton concentration changes corresponds to a limited pH value change of 0.3, the unique simplicity of the discovered *in situ* Raman spectroscopic method in measuring near-surface acidity changes set it apart from the near-surface acidity measurement methods available in the literature.

Acknowledgements: This work was supported by a grant from DOE-BES (DE-FG02-07ER15895).

Notes and references

Department of Chemistry, Georgetown University, 37th & O Streets, NW, Washington, DC 20057. Email: yyt@georgetown.edu.

Electronic Supplementary Information (ESI) available: [details of any supplementary information available should be included here]. See DOI: 10.1039/c000000x/

1. Y.-F. Yang and G. Denuault, *Journal of the Chemical Society, Faraday Transactions*, 1996, **92**, 3791-3798.
2. L. W. Liao, M. F. Li, J. Kang, D. Chen, Y.-X. Chen and S. Ye, *Journal of Electroanalytical Chemistry*, 2013, **688**, 207-215.
3. F. King, C. D. Litke and Y. Tang, *Journal of Electroanalytical Chemistry*, 1995, **384**, 105-113.
4. N. García, V. Climent, J. M. Orts, J. M. Feliu and A. Aldaz, *ChemPhysChem*, 2004, **5**, 1221-1227.
5. J. Joo, T. Uchida, A. Cuesta, M. T. M. Koper and M. Osawa, *Journal of the American Chemical Society*, 2013, **135**, 9991-9994.
6. S. Strbac and R. R. Adzic, *Electrochimica Acta*, 1996, **41**, 2903-2908.
7. Y.-F. Yang and G. Denuault, *Journal of Electroanalytical Chemistry*, 1998, **443**, 273-282.
8. B. C. H. Steele and A. Heinzel, *Nature*, 2001, **414**, 345-352.
9. S. Wasmus and A. Kuver, *Journal of Electroanalytical Chemistry*, 1999, **461**, 14-31.
10. A. A. Gewirth and M. S. Thorum, *Inorganic Chemistry*, 2010, **49**, 3557-3566.
11. E. Klusmann and J. W. Schultze, *Electrochim. Acta*, 1997, **42**, 3123-3134.
12. Y.-F. Yang and G. Denuault, *J. Chem. Soc., Faraday Trans.*, 1996, **92**, 3791-3798.

13. W. J. Albery and E. J. Calvo, *Journal of the Chemical Society, Faraday Transactions 1: Physical Chemistry in Condensed Phases*, 1983, **79**, 2583-2596.
14. P. Steegstra and E. Ahlberg, *Journal of Electroanalytical Chemistry*, 2012, **685**, 1-7.
15. L. Lawson and T. Huser, *Analytical Chemistry*, 2012, **84**, 3574-3580.
16. X.-S. Zheng, P. Hu, Y. Cui, C. Zong, J.-M. Feng, X. Wang and B. Ren, *Analytical Chemistry*, 2014, **86**, 12250-12257.
17. J. Kneipp, H. Kneipp, B. Wittig and K. Kneipp, *Nano Letters*, 2007, **7**, 2819-2823.
18. S. W. Bishnoi, C. J. Rozell, C. S. Levin, M. K. Gheith, B. R. Johnson, D. H. Johnson and N. J. Halas, *Nano Letters*, 2006, **6**, 1687-1692.
19. J. O. M. Bockris and A. K. N. Reddy, *Modern Electrochemistry: Ionics*, 2nd edn., Plenum Press, New York and London, 1998.